

EVALUATION THE SENSITIVITY OF TiO₂ DOPED Al IN GLUCOSE SOLUTION

G. A. GHAZWAN*, M. H. YOUNUS, L. R. MUHAMMED

*Department of Physics, College of Education for Pure Science, Mosul University,
Mosul, Iraq*

Aluminum (Al) deposited on Titanium dioxide (TiO₂) thin films under different dose (10¹⁰, 10¹¹ and 10¹²) ion/cm² have been prepared as a wave guide sensor using DC reactive sputtering technique on glass substrates and then compared to un deposited Al thin film .The structure, morphological and optical properties of Al: TiO₂ films have investigated by XRD, SEM and UV-VIS spectrophotometer. These results show that peaks intensity of XRD patterns increases with increasing of Al dose . Furthermore, The crystalline phase of TiO₂: Al has tetragonal structure of anatase and rutile phase. SEM images illustrate irregular distribution with worm like shape. The absorbance increases with increasing of Al dopant dose while the energy gap decreased. This leads to enhance of sensitivity of TiO₂:Al thin film. Moreover, the sensitivity of TiO₂ sensor after Al dopant dose has increased to detect different concentration of glucose solution. It can be seen, the maximum sensitivity of 20.3 dB/ con. is achieved at dose 10¹² ion/cm². Then, Titanium dioxide and doped with Al dose are good performance applications specially in biochemical and biological detection.

(Received August 31, 2019; Accepted December 9, 2019)

Keywords: Titanium dioxide, Chemical sensors, Sputtering, Waveguide sensor

1. Introduction

The Titanium dioxide was discovered in the beginning of 1971 by William Gregor [1]. TiO₂ thin film has an attractive application such as electronic and optical devices due to its high dielectric constant high refractive index [2]. TiO₂ thin films have different applications, such as anti-reflection coatings and optical filters [3,4]. Several papers have received considerable attention for photo-catalytic properties of TiO₂ thin film [5,6]. The properties can be changed by using different types of dopants like Al [7,8]. The TiO₂ thin film has unique properties such as excellent optical properties , non-toxicity, low cost , and large band gap [9,10]. The methods of the thin films have been used to prepare TiO₂ films such as sputtering [11] ,sol -gel [12], and chemical vapor deposition CVD [13]. solution precursor chemical vapor deposition (SPCVD) [14]. Reactive sputtering is preferable because high deposition rates can be obtained at low substrate temperature [15]. Reactive sputtering is a technique widely used in the electronics industry to produce thin films of metals, semiconductors, and insulators on solid substrates from volatile reagents [16,17]. Recently , ion implantation technique is preferred over many techniques because low temperature process and accurate dose control [18, 19]. The scientific community has increased growing energy to enhance the light applications [20] .The aim of this work is enhancement the sensitivity of TiO₂ thin film. Hence, we study effect of Al doping dose on structural, morphological and optical properties of TiO₂ thin film using reactive sputtering.

*Corresponding author: dr.ghazwan39@yahoo.com

2. Experimental part

Titanium oxide thin films have deposited on glass substrate by DC reactive sputtering method. Ion implantation technique has been used for doping Al ions on the surface of TiO₂ thin films by different dose (10¹⁰, 10¹¹ and 10¹²) ion/cm² and fixed energy 40 KeV . The target system was cooled with water to 5 °C. After coated , the samples keep inside the sputtering chamber in

order to cool down slowly under vacuum and then the cover of vacuum opened. The setup of waveguide sensor coated Al on TiO₂ substrate with different Al dose is used to detect different glucose concentration is observed in Fig. 1. The set up contains a semiconductor laser source (USA Stellar, Net, Inc. Model SL.2,) with wavelength 650 nm and photo-detector with a extremely sensitive (EPT-2200, Stellar Net Inc., USA) with spectral response from (100 - 1200) nm. The laser source emits the signal over the waveguide sensor after its exposing of glucose solution of various concentration and photo-detector detects transmitted signal . Furthermore, The laser source, waveguide sensor , photo-detector, and the two lenses were all located together to give the high signal received by the photo-detector using 3D micro positioners. The waveguide coated with TiO₂:Al was immersed on a cell filled with the solution, then the incident light source passes across the cell and the light of output were transmitted into the detector.

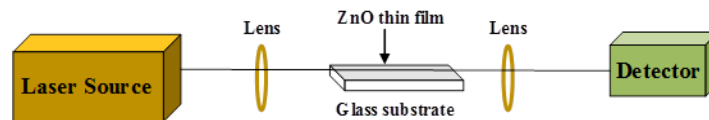


Fig. 1. setup of waveguide sensor.

3. Results and discussion

3.1. Structure properties

The XRD of un-deposited and Al- deposited on TiO₂ substrate with various dose (10¹⁰, 10¹¹ and 10¹²) ion/cm² shows as Fig. 2. The crystal structure of TiO₂: Al has tetragonal structure of anatase and rutile phase . The maximum peak (101) corresponds at 2φ= 26.188° of anatase of un-deposited Al dose. In the other hand , we note appearance of new peaks with increase Al dopant dose such as (110) at 2φ= 28.446° of rutile phase also small peaks as (230) represent the bonds Al₂TiO₃ and (200) AlTiO₃, (200) ,and (221) correspond 2φ= 33.253° , 36.085° , 39.050° , and 54.640° respectively as Fig.2 , this is agreement with JCPDS Card [21]. The structure of TiO₂:Al depends on growth process of the Al dose thin films from anatase to rutile, due to rutile is the most stable form of TiO₂. Furthermore, the deposited atoms (ions) have lost most of their energy by collisions with other ions and atoms species in the vacuum . Moreover, crystal structure of thin film depends on the Al dose dopant . It can be seen , increase of the Al does thin films lead to increase the peak intensity. crystalline size can be calculated by using the Scherer equation [22]:

$$D = \frac{k\lambda}{B\cos\theta} \quad (1)$$

Where λ is the beam of the X-ray wavelength (0.154606 nm), θ : is the angle of scattering, D is grain size (nm) , ($k=0.89$) and (B) is FWHM.

Table 1. Shows the crystalline sizes with different dose .

Al dose (ion/cm ²)	Grain Size (nm)
Un- coated	12.76
1×10 ¹⁰	17.51
1×10 ¹¹	21.65
1×10 ¹¹	23.24

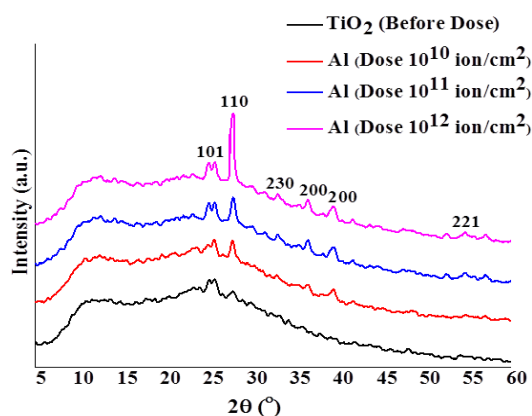


Fig. 2. XRD patterns of Al: TiO₂ of different dose.

3.2. Surface morphology

Scanning electron microscope (top surface and cross section) is used to study the surface morphology of un-deposited and Al- deposited on TiO₂ substrate with various dose. It can be seen that the image of dose 1×10¹⁰ ion/cm² of Al has homogeneous distribution in shape compared with other dose as Figure 3a . It can be noted that the surface of dose 1×10¹¹ and 1×10¹² ion/cm² of Al :TiO₂ have irregular distribution with worm – like shape as Fig. 3 (b and c) [23]. It has been observed that increasing of deposited Al leads to increase the crystallite growth . On the other word, the crystallite size increases with increasing Al dose, due to decrease the number of surface particles by the Aluminum dissolution in TiO crystal lattice as Fig.4.(a,b, and c) [24].

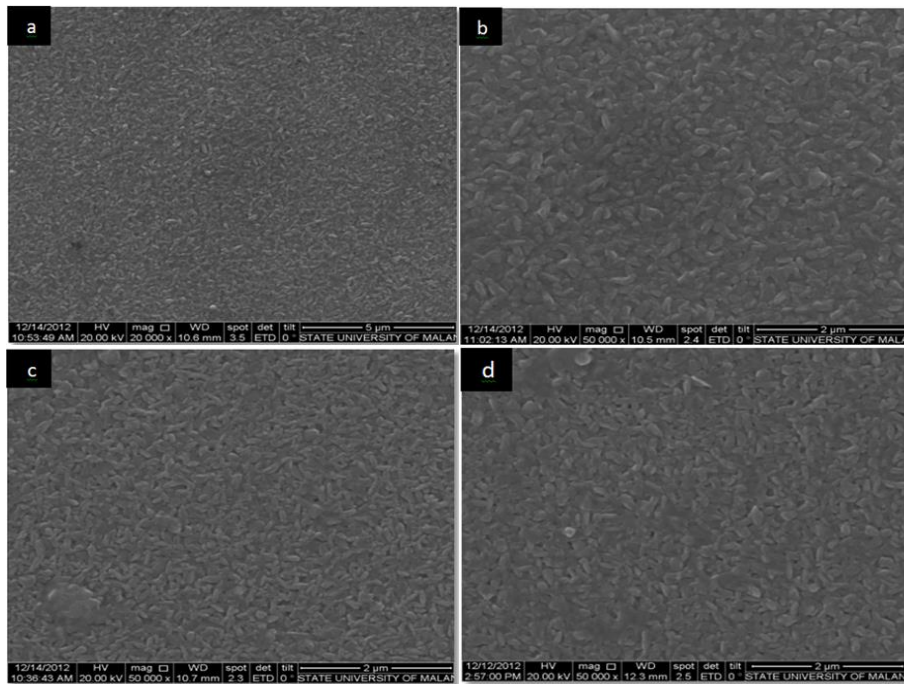


Fig. 3. SEM (Top surface) of Al: TiO₂ of dose (a) un-dopant Al, (b) 10^{10} ion/cm², (c) 10^{11} ion/cm², (d) 10^{12} ion/cm².

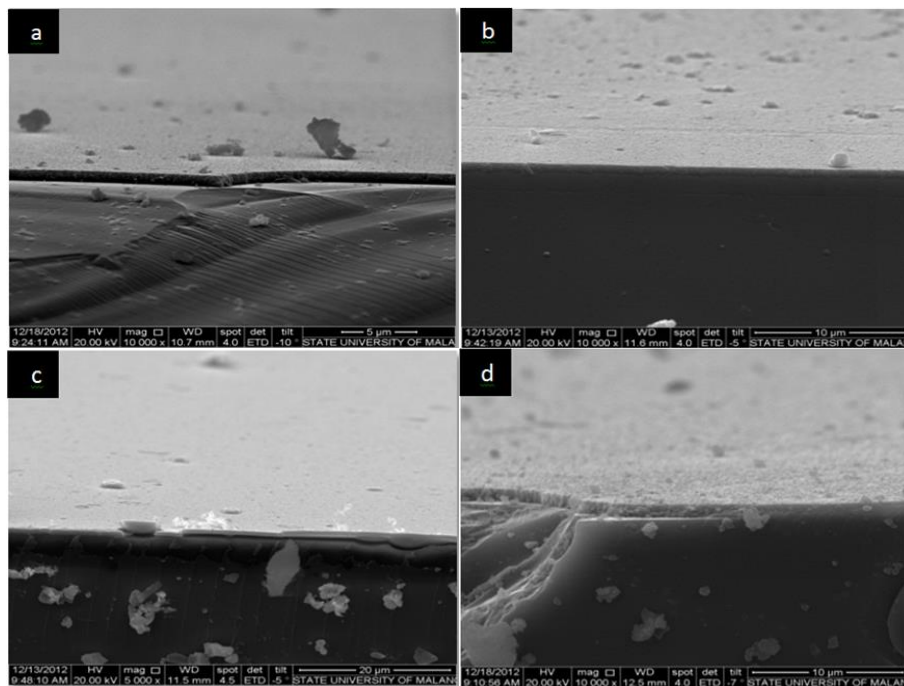


Fig. 4. SEM (cross section) of Al: TiO₂ of dose (a) un-dopant Al, (b) 10^{10} ion/cm², (c) 10^{11} ion/cm², (d) 10^{12} ion/cm².

3.3 Optical properties

The study of optical properties demonstrated that optimizing the content and placement of the Al dopant ions content play a positive role in affecting of sensitivity , and then enhancement of visible light absorption [25]. Fig. 5 illustrates strong absorption spectra of TiO₂: Al . Furthermore, the absorbance spectra of Al-TiO₂ increase with increasing Al dopant dose , this is

leading to enhance the capture of incident light [26]. The maximum absorbance is observed by dose 1×10^{12} ion/cm² of Al dopant due to electron-hole recombination can occur as well as the hole-donor and electron-acceptor surface of the semiconductor are quenched. electron-transfer resulting in the release reactions of light [27,28].

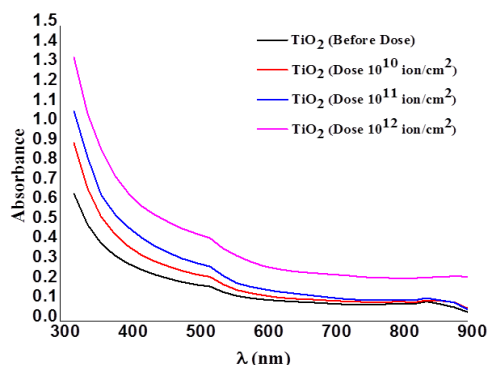


Fig. 5. Absorbance vs. wavelength at different dose.

The optical band gap decreases with increasing of Al dopant dose due to the formation of a non-stoichiometric material with increasing oxygen vacancies [29]. The values of energy gap were about (3.21 to 3.02) as shown in Fig. 6.

Energy gap was evaluated by the following equation [30]:

$$\alpha h\nu = B(h\nu - E_g)^r \quad (2)$$

Where r is equal 2 of indirect transition and $1/2$ of direct transition, and equals. B is constant, $h\nu$ is the photon energy and α is the absorption coefficient.

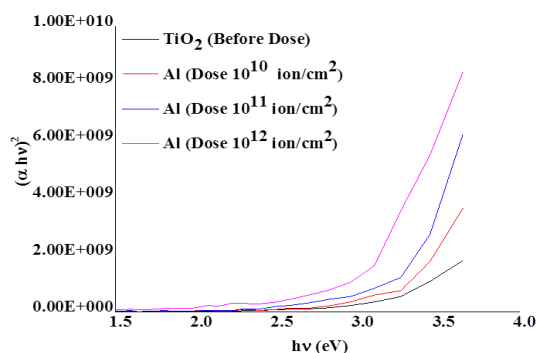


Fig. 6. $(\alpha h\nu)^2$ vs. $h\nu$ (eV) at different dose.

The optical constants can be calculated dependence on the wavelength as extinction coefficient, and dielectric constant (real part ϵ_r and imaginary part ϵ_i). It can be seen that the extinction coefficient increases linearly with Al dopant dose as Fig. 7.

The extinction coefficient is related to the absorption coefficient by equation [31]:

$$k = \frac{\alpha\lambda}{4\pi} \quad (3)$$

Furthermore, the real part ϵ_r decreases gradually with Al dopant dose, while the imaginary part ϵ_i increased as Figs. 8 and 9 [32]. Where the dielectric constant can be introduced by [33]:

$$\epsilon = \epsilon_r - i\epsilon_i \tag{4}$$

The real part ϵ_r and imaginary part ϵ_i are calculated by [34]:

$$\epsilon_r = n^2 - k^2 \tag{5}$$

$$\epsilon_i = 2nk \tag{6}$$

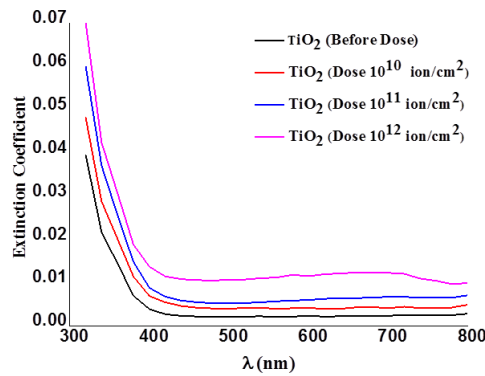


Fig. 7. Extinction coefficient vs. wavelength at different dose.

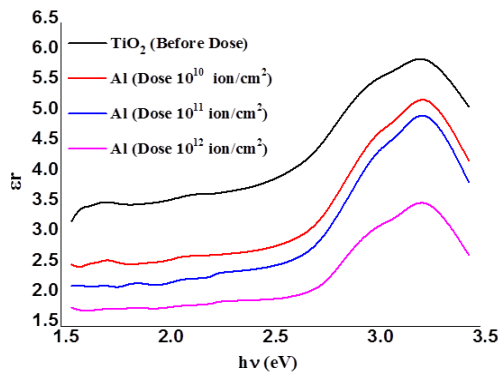


Fig. 8. Real part vs. photon energy at different dose.

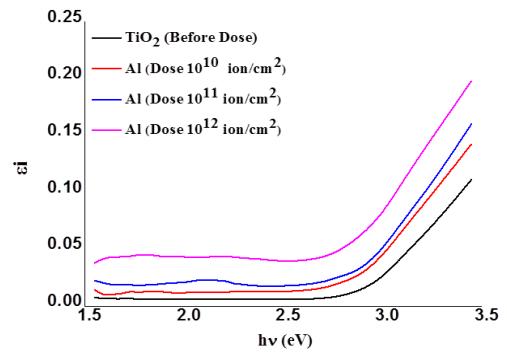


Fig. 9. Imaginary part vs. photon energy at different dose.

3.4. Sensitivity measurement of waveguide sensor

Fig. 10 shows the optical losses versus glucose concentrations before and after irradiation with Al ion dose. The responses of fabricated TiO₂:Al based glucose sensors were in the concentration range of 0.01 to 0.05, measured in dose range of 10¹⁰, 10¹¹ and 10¹² ion/ cm². As one can see from the Figure 10, the optical losses increases in linear line as the glucose concentration is increased of all ion dose values. The sensitivity determined from the linear slope in the Figure 10, was found to be dependent on ion dose level. For high ion dose (10¹² ion/ cm²), the sensitivity was as high as 20.3 (dB/con.), while at low ion dose (10¹⁰ ion/ cm² and 10¹¹ ion/ cm²), the sensitivities were about 12.337 (dB/con.) and 16.7 (dB/con.) respectively. Fig. 11 presents the sensitivity versus ion doses of TiO₂:Al thin films towards glucose solution. As shown in Figure

11, the results showed that the sensitivity of prepared TiO₂:Al thin films increases as the ion dose is increased which indicated the high selectivity and applicability for detection in different fields.

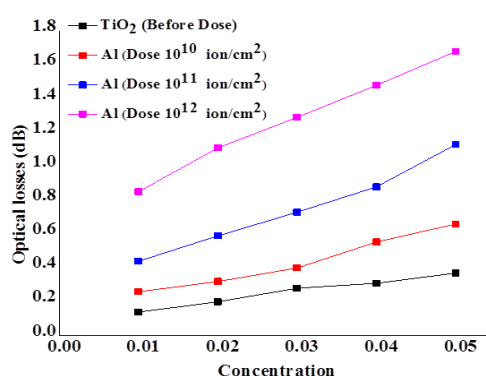


Fig. 10. The optical losses of TiO₂:Al thin film versus glucose concentration.

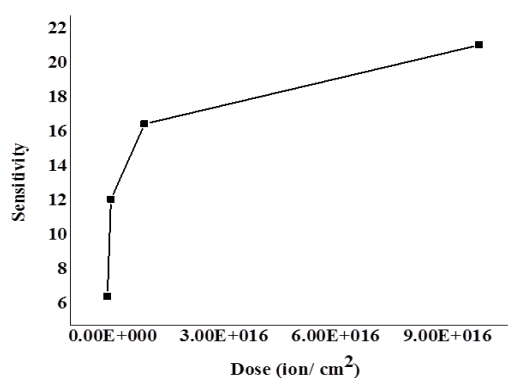


Fig. 11. The sensitivity of TiO₂: Al thin film versus. the ion dose.

4. Conclusion

The waveguide sensor was synthesized and characterized by Aluminum (Al) deposited on Titanium dioxide (TiO₂) thin films on the glass substrates. The structure, optical and morphological properties using ion implantation technique were enhanced the sensitivity of TiO₂:Al thin films. The crystalline sizes dependence on Al dopant dose. The crystalline phases of TiO₂: Al have various energy gap from anatase to rutile band gap (3.21 to 3.02) eV. Additionally, the waveguide sensor is a good sensitivity for the solution of glucose with increment of aluminum doping dose. Hence, the best value of sensitivity was 20.3 dB/con. of TiO₂:Al with dose 1×10^{12} ion/cm² and then well improved sensitivity performance. While the lower sensitivities were 6.33, 12.337, and 16.7 dB/con. of TiO₂, 1×10^{10} ion/cm² and 1×10^{11} ion/cm² respectively.

References

- [1] B. Liu, J. Yang, Zhao, X.; Yu, J., Phys. Chem. **19**, 8866 (2017).
- [2] S. A. Ansari, Khan, M. M. Ansari, M. O. Cho, New J. Chem. **40**, 3000 (2016).
- [3] M. Niu, R. Cui, H. Wu, D. Cheng, D. Cao, J. Phys. Chem. **119**, 13425 (2015).
- [4] M. Zahid, E. L. Papadopoulou, G. Suarato, V. D. Binas, G. Kiriakidis, I. Gounaki, O. Moira, D. Venieri, I. S. Bayer, A. Athanassiou, ACS Appl. Bio Mater. **1**, 1154 (2018).
- [5] P. Zhang, T. Tachikawa, M. Fujitsuka, T. Majima, Chem Sus Chem **9**, 617 (2016).

- [6] M. R Parra, P. Pandey, H. Siddiqui, V. Sudhakar, K. Krishnamoorthy, F. Z. Haque, Appl. Surface Sci. **470**, 1130 (2019).
- [7] S. Yun, Y. A. R. Qin, N. Uhl Vlachopoulos, M. Yin, D. Li, Ener. and Envir. Sci. **11**, 476 (2018),
- [8] M. Ye, C. Chen, M. LV, D. Zheng, W. Guo, C. Lin , Nanoscale **5**, 6577 (2013).
- [9] J. Luo, J. Zhou, H. Guo, W. Yang, B. Liao, W. Shi, RSC Advances. **4**, 5631 (2014).
- [10] F. W. Low, C. W. Lai, S. Hamid, Ceram. Inter. **431**, 625 (2017).
- [11] Y. H. Peng, G. F Huang, W. Q Huang, Adv. Powder Tech. **23**, 8 (2012).
- [12] Y. Li, W. Wang, X. F. Qiu, L. Song, H. M. Meyer, M. P. Paranthaman, G. Eres, Z. Y. Zhang, B. H. Gu, Appl.Catalysis B: Environmental **110**, 148 (2011).
- [13] J. C. Colmenares, A. Magdziarz, K. Kurzydowski, J. Grzonka, O. Chernyayeva, D. Lisovtyskiy, Appl. Catalysis B: Environmental **13**(5), 136 (2013) .
- [14] S. Chen, Y. Wang, J. Li, Z. Hu, H. Zhao, W. Xie, Z. Wei, Mater. Res. Bull. **98**, 280 (2018).
- [15] M. Rahman, M. Kaiyum, M. Islam, J. of Thin Films Research **1**(1), 17 (2017).
- [16] N. Said, M . Sahdan, A. Ahmad, American Inst. of Phys. **1788**, (2017).
- [17] Y. Song, B. Kim, N. Cho, J. of Nanosci. and Nanotechno. **15**(2), 5228 (2015).
- [18] N. Zainab Jameel, Synthesis of TiO₂ Nanoparticles by Sol-Gel Method using Laser Ablation for nano paint Application, PhD thesis, University of Baghdad, Physics Department, (2015).
- [19] J. Adawiya, N. Zainab, Y. Samar, Eng. & Tech. Journal **33** part (B), 5 (2015).
- [20] M. Farahmandjou, P. Khalili, Australian J. Basic Appl. Sci. **7**(6), 462 (2013).
- [21] H. E. Swanson, E. Tatge, J. Res. Natl. Bur. Stand. **46**, (1951).
- [22] F. Bensouici, M. Bououdina, A. Dakhel, T. Souier, R. Tala-Ighil, M. Toubane, Thin Solid Films **616**, 655 (2016).
- [23] Z. Johannes, M. Ziyanda, J. of Mater. Sci.& Eng. **8**(1), (2019).
- [24] J. Bani Fathima Sharfudeen, L. Afrin, V. Rose, J. Pharm. Sci. & Res. **9**(9), 1604 (2017),
- [25] J. Adawiyah, N. Zainab, H. Imad, Techn. and Mater. for Renew. Energy, Envir. and Sustainability, Energy Proc. **157**, 17 (2019).
- [26] L. Kernazhitsky, S. Valentyna, G. Tatiana, Journal of Physics and Chemistry of Solids **126**, 234 (2018).
- [27] C. Shyniya, B. Amarsingh, T. Rajasekaran, J. of Mater. Sci. Mater. in Electro. **28**(9), (2017).
- [28] M. Evtushenko, S. Romashkin, N. Trofimov, T. Chekhlova, Phy. Proc. **73**, 100 (2015) .
- [29] S. Anton, I. Poluboyarinov, V. Chelpanov, A. Vasily , Mater. **12**, 1472 (2019).
- [30] X. Kefeng, J. Qiangqiang, W. Yizhe, Z. Wenxue, X. Jingcheng, Mater. **11**, 179 (2018).
- [31] I. Sta, M. Jlassi, M. Hajji, F. Boujmil, R. Jerbi, M. Kandyla, M. Kompitsas, J. of Sci. and Tech. **72**, 421 (2014).
- [32] T. Venkatachalam, K. Sakthivel, R. Renugadevi, R. Narayanasamy, P. Rupa, AIP Conf. Proc. **1391**, 764 (2011).
- [33] Z. Essalhi, B. Hartiti, A. Lfakir, M. Siadat, P. Thevenin, J. Mater. Environ. Sci. **7**(4), 1328 (2016).
- [34] V. Andrey, N. Konstantin, V. Dzyuba, N. Kulchin, Asia-Paci. Conf. on Fundamental Problems of Opto- and Microelectronics **3**, 2017.